International Journal of Microwave and Wireless Technologies

cambridge.org/mrf

Design and implementation of 2.5D frequency-selective surface based on substrate-integrated waveguide technology

Krushna Kanth Varikuntla and Raghavan Singaravelu

Department of Electronics and Communication Engineering, National Institute of Technology Tiruchirappalli, Trichy, India

Research Paper

Cite this article: Varikuntla KK, Singaravelu R (2019). Design and implementation of 2.5D frequency-selective surface based on substrate-integrated waveguide technology. *International Journal of Microwave and Wireless Technologies* **11**, 255–267. https://doi.org/10.1017/S1759078718001678

Received: 5 July 2018
Revised: 10 December 2018
Accepted: 12 December 2018
First published online: 10 January 2019

Key words:
EM field theory and numerical techniques; microwave measurements; modeling and measurements; wave propagation and scattering

Author for correspondence:
Krushna Kanth Varikuntla, E-mail: krushnakanthv@gmail.com

Abstract

In this paper, the patch-type frequency selective surfaces (FSS) based on substrate-integrated waveguide (SIW) technology is proposed to improve the bandwidth (BW) and angular performance. The proposed FSS configuration overcomes the limitations of both conventional 2D and 3D FSS structures. A closely coupled cascaded mechanism is employed to combine two identical FSS elements separated by thin dielectric substrate results in incorporation of SIW technology; hence, named as 2.5D FSS. A derived equivalent circuit model is used to estimate the basic performance of proposed FSS–SIW elements, and the response of analytical expressions has been validated and final design is obtained using full-wave simulations. Two basic FSS elements viz. single square loop and a Jerusalem cross have been investigated to prove the enhancement in their BW and angular stability. The proposed technique evidently improves the BW and angular stability of FSS structures than in its established form. Besides, various important parameters that influence the performance characteristics of reported 2.5D FSSs are also studied. The important observations made on the thickness, as the thickness increases the bandstop FSS, can change to bandpass FSS. Finally, the proposed FSS structure has been fabricated and measured using free space measurement setup, to show the effectiveness of theoretical results. The measured results show good agreement with simulated results at normal and oblique incidence angle.

Introduction

Frequency-selective surfaces (FSSs) are thin periodic pattern designed to filter electromagnetic (EM) waves based on the frequency range of interest [1]. It might be a single, double, multi, or broadband [2–6]. In this sense, FSS is a virtue of regular 2D periodic array designed over a substrate material, usually metallic, sometime dielectric [7, 8]. These surfaces found their potential applications in the design of antenna sub-reflectors, artificial magnetic surfaces, high-impedance surfaces, side walls of microwave oven to prevent the EM field leakage, radomes, radar-absorbing structures, and modern metamaterials [9].

Though not explicitly mentioned in the name, FSSs also have properties which may vary with incidence angle and polarization as well. These are unavoidable consequences of the way in which conventional FSSs are constructed. Moreover, the applications of 2D FSSs are limited because of its narrowband and unstable response. A miniaturized FSS elements have been reported in the open literature for stable resonance performance [10, 11]. Aforementioned, elements may disintegrate at higher power levels and loss their basic functioning [12, 13]. The periodic surfaces, used in microwave applications, are continuously exposed to high average powers. Hence, the lossy materials will develop heat and result in melt/burn of conducting patterns. Moreover, very high electric fields will develop in the patch or slot elements. It will induce arcing effect that makes the surface short-circuited and non-operational. Increasing the gap between unit cells and thickness of substrate is one of the solutions to this problem. However, only moderate improvement is possible with this approach [1]. It is well known that the high-power handling and bandwidth (BW) can be achieved using thick metal but it leads to a bulkier structure.

The aforementioned limitations of 2D FSS can be overcome by using multilayered or 3D FSS structures [14, 15]; whereas, the structural complexity is improved. Moreover, weight of the structure increased. The increased weight and payload make them unsuitable for many real-time and aerospace applications. A concept of series vais has been used in SOI to reduce the cross talk [16]. The substrate-integrated waveguide (SIW) technology has been introduced into FSS design for better performance (high Q-factor) by upholding the unit-cell properties when it is used as an infinite surface without altering its resonant characteristics [17]. It can also show a stable response w.r.t the angle of incidence [18, 19]. Hence, it is believed that the FSS structures using SIW technology can overcome the limitations of both 2D (instability) and

© Cambridge University Press and the European Microwave Association 2019

CAMBRIDGE UNIVERSITY PRESS

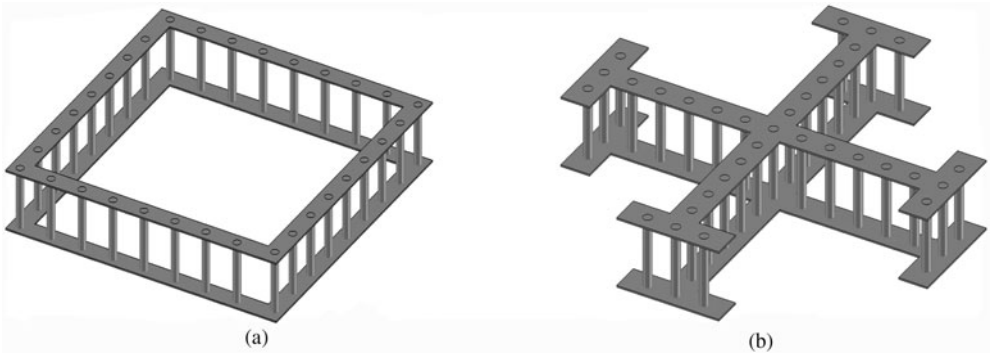


Fig. 1. Geometry of proposed 2.5D FSS unit cell based on SIW (substrate is hidden to show the structure clearly): (a) square loop, (b) Jerusalem cross (substrate has been hidden to show the structure clearly).

3D (weight) FSS structures and work as 2.5D FSS structure. The EM performance of FSS elements has been improved and enhanced passband characteristics have been achieved by using SIW technology [20, 21]. Recently, an FSS with narrow band configurable polarization rotator with minimal insertion loss is demonstrated using the concept of SIW technology [22].

As of now, the researchers developed slot-type FSS based on SIW technology to improve its performance. When dealing with the patch-type FSS, creating vias around the unit element leads to the formation of another resonance which disturbs the original performance of unit cell. To overcome this limitation, a novel design is reported in this paper. The design procedure of proposed structure is explained in further section. So far, the complex numerical techniques such as finite difference time domain (FDTD) method, MoM/Bi-RME, and commercial simulation software packages have been used to analyze this type of structures, which may take more computation time to execute the problem [17, 23].

In this paper, a single square loop (SSL), a loop type, and a Jerusalem cross (JC), a center-connected type elements, have been chosen to prove the enhancement in their stopband and stable response using SIW technology. The structures are designed to resonate at 10 GHz by considering its tremendous applications in civil, military radars, air traffic control and defense tracking. An equivalent circuit (EC) model is derived for both chosen elements to analyze the structural response. The described ECM technique can closely predict the transmission and reflection characteristics at a normal and oblique angle of incidence for both parallel (TE) and perpendicular (TM) polarizations. Further, the proposed technique can eliminate undesirable coupling between adjacent FSS elements. Moreover, the designed FSS will act as a virtually thick screen, which may be useful for high-power handling. Finally, the results obtained using the derived EC model is verified with the help of full-wave simulation (FDTD-based commercial simulation package CST Microwave Studio (CST MWS)) and measured results.

EM design of FSS–SIW element

Generally, conventional FSS array is printed on one side of a dielectric substrate. In this work, a 2.5D FSS is implemented using the SIW concept. To facilitate, two identical FSS elements are printed on top and bottom side of a thin dielectric substrate (thickness, $t \leq \lambda_{eff}/4$ where $\lambda_{eff} = \lambda_0/\sqrt{\varepsilon_r}$) and connected by means of thin metallic vias (series of thin cylinders) results in incorporation of SIW concept in FSS design. In this study, two kinds of FSS elements viz. a SSL and a JC which are examples of loop-type and center-connected FSS elements, respectively, have been chosen for further investigations. Figures 1(a) and 1(b) illustrate the unit-cell models of improved FSS structure based on SIW technology. In loop-type FSS, the proposed concept will resemble the Faraday cage. The FSS elements printed on both sides of dielectric substrate act as a parallel combination of L, C equivalent tank circuit. Metallic vias will act as an inductive element (Lvia) connected in series and small intrinsic capacitive effects (Cvia) due to the dielectric spacer is connected in parallel to Lvia. The modified equation of ε_{eff} [24] has been used in the EC model to estimate the scattering performance of the structures with low estimation error. It is worth to mention that in [24] authors presented the rigorous analysis to optimize the EC models. However, this work is different from the conventional FSS elements. The proposed FSS elements consist of two layers strongly connected through metallic vias. The structure has a very stable performance and higher BW compared with the FSS in its established form. In addition, it presented the EC models to analyze the structure response. The via has been modeled as an inductance, and the gap between two FSS elements is modeled as mutual capacitance. The transmission line approach is used to evaluate the total impedance and scattering characteristics of the structure.

Square loop

The pictures presented in Figs 2(a) and 2(b) show a unit-cell geometry and its corresponding EC model of a conventional SSL FSS, respectively. The same element is considered for showing the SIW technology with interconnected metallic vias from top FSS layer to bottom FSS layer and its improved EC model shown in Figs 2(c) and 2(d). The final design dimensions of SSL FSS are: periodicity $p = 9.25$ mm which corresponds to $\approx 0.308\lambda_0$ (λ_0 be the free space wavelength at 10 GHz), $d =$ 7.5 mm, $s = 0.6$ mm. The gap between two adjacent unit cells is g, which is equal to (p–d). The diameter and center to center spacing of metallic vias are D_via = 0.4 mm and K_via = 0.635 mm, respectively. The conducting metal patches of FSS are made of copper coating with a metal thickness of microns. The L and C values of square loop have been computed by its EC model given in equation (1)–(5). EC model offers an easy and quick method in FSS analysis. It serves as a good alternative to EM simulation.

$$\text{For TE, } X_L = \omega L = \left(\frac{d\cos\theta}{p}\right) \cdot F(p, 2s, \lambda, \theta), \qquad (1)$$

https://doi.org/10.1017/S1759078718001678 Published online by Cambridge University Press

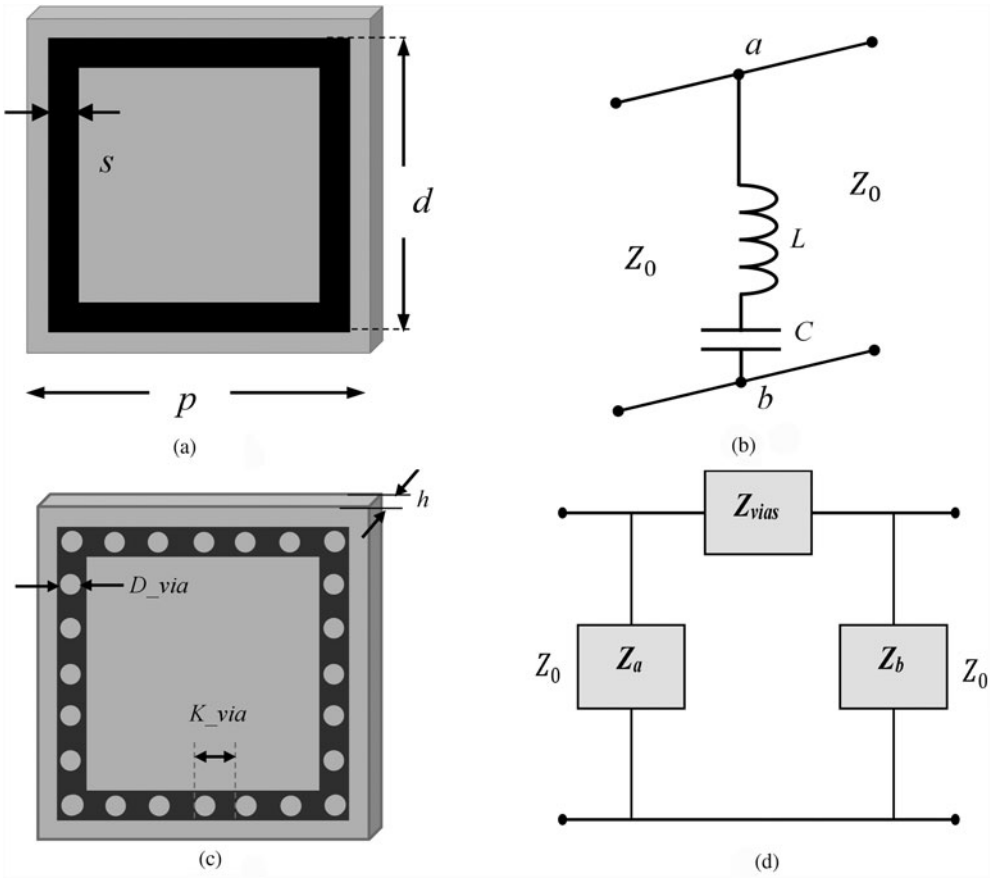


Fig. 2. Square loop FSS unit-cell geometry: (a) SSL, (b) equivalent circuit model, (c) 2.5D SSL–SIW, (d) improved equivalent circuit model.

$$B_C = \omega C = 4 \cdot \varepsilon_{eff} \cdot \left(\frac{d \sec\theta}{p}\right) \cdot F(p, g, \lambda, \theta), \tag{2}$$

$$\text{For TE, } X_L = \omega L = \left(\frac{d \sec\phi}{p}\right) \cdot F(p, 2s, \lambda, \phi), \tag{3}$$

$$B_C = \omega C = 4 \cdot \varepsilon_{eff} \cdot \left(\frac{d \cos\phi}{p}\right) \cdot F(p, g, \lambda, \phi), \tag{4}$$

where ε_{eff} is the effective dielectric constant. $F(\cdot)$ is a function of design variables p, s, d, g and incident angle (θ, ϕ) depends on polarization which is given as:

$$F(p, w, \lambda, \theta) = \frac{p}{\lambda}\left[\ln\left(\csc\frac{\pi w}{2p}\right) + G(p, w, \lambda, \theta)\right]. \tag{5}$$

In above equations, $G(\cdot)$ is the correction term given in [24].
In Fig. 2(d), Z_a and Z_b correspond to impedances offered by the top and bottom FSS layers ($Z_a = Z_b = Z_{FSS}$), respectively, which are computed by L and C. Z_{vias} is the impedance offered by the inductive posts connected to both FSS elements which is explained in the next section.

Jerusalem cross

JC is one of the classical elements used in FSS analysis [25]. Hence, it is chosen as an example of center-connected FSS element. Figures 3(a) and (b) shows a unit-cell geometry and its corresponding EC model, respectively; whereas, Figs 3(c) and 3(d) show the proposed structure and its EC model successively. The final design dimensions of JC FSS are: $p = 9.25$ mm which corresponds to period of element. Arm's length of JC is $d = 2.3$ mm and the width of JC cross and arm is $w = t = 0.65$ mm. The gap between two adjacent unit cells is g, which is equal to (p–d). The proposed structure is analyzed on R04003C substrate with $\varepsilon_r = 3.38$ having a thickness $h = 0.81$ mm. The L and C of JC element is computed by Equations (6)–(9) [25].

$$\text{For TE} : X_L = \omega L = \left(\frac{p \cos\theta}{d}\right) F(p, w, \lambda, \theta), \tag{6}$$

$$B_C = \omega C = 4 \cdot \varepsilon_{eff} \cdot F(p, g, \lambda, \theta), \tag{7}$$

$$\text{For TM} : X_L = \omega L = \left(\frac{p \sec\phi}{d}\right) F(p, w, \lambda, \phi), \tag{8}$$

$$B_C = \omega C = 4 \cdot \varepsilon_{eff} \cdot F(p, g, \lambda, \phi), \tag{9}$$

https://doi.org/10.1017/S1759078718001678 Published online by Cambridge University Press

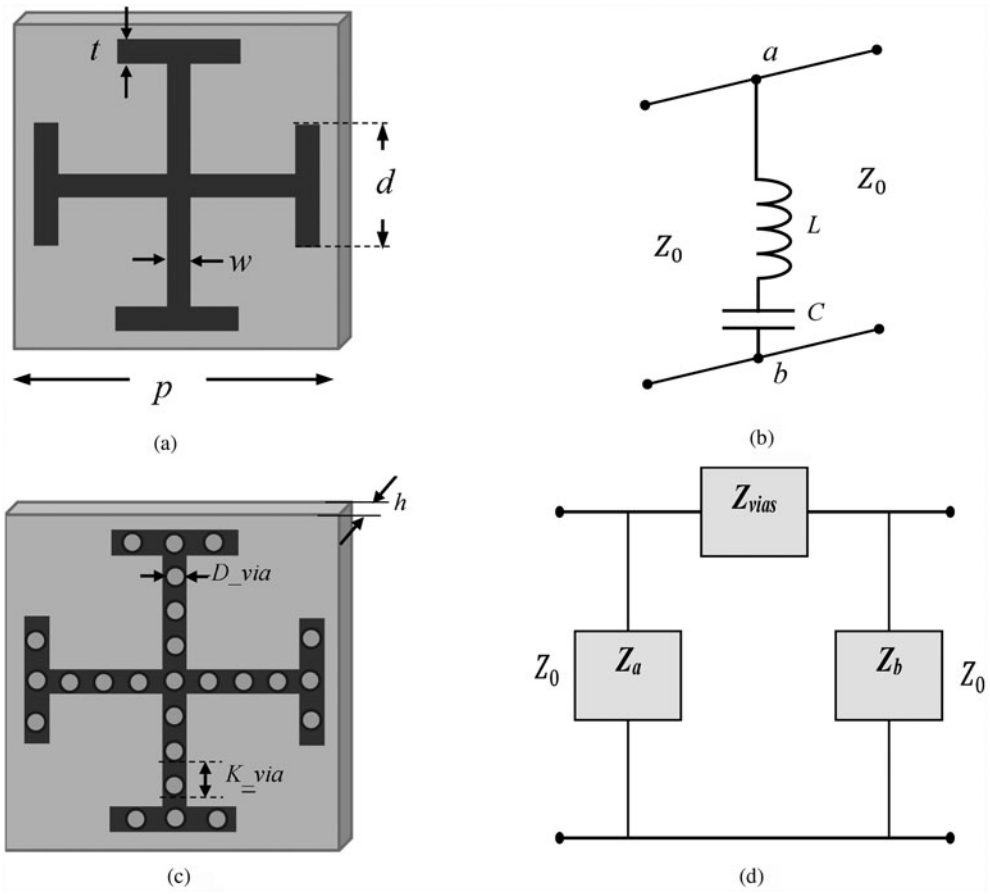


Fig. 3. Jerusalem cross FSS unit-cell geometry: (a) JC FSS, (b) equivalent circuit model, (c) 2.5 D JC–SIW, (d) improved equivalent circuit model.

where $F(\cdot)$ and $G(\cdot)$ are function of design variables and correction term, respectively, as described in the previous section. The dielectric effects of substrate material have been considered for better estimation of the resonance characteristics. In the proposed EC model, the classical ε_{eff} has been replaced with the improved empirical model. Equation (10) gives better approximation than ε_{eff} when used for the computation of capacitance.

$$\varepsilon_{corr} = \frac{\varepsilon_r + 1}{2} - \frac{\varepsilon_r - 1}{2} \cdot e^{(-13h/p)} - \left(\frac{100s^2}{d} - 2g + 10h\right) \mathrm{m}^{-1}. \quad (10)$$

The normalized impedance w.r.t free space impedance ($Z_{FSS} = Z_a = Z_b$) offered by conventional SSL and JC FSS elements is computed by the EC models based on the lumped elements induced by the structure [24, 25]:

$$Z_{FSS} = j\left(\frac{X_g}{1 + jX_g}\right), \quad (11)$$

where X_g is the reactance offered by the grid elements which is expressed as:

$$X_g = \left(X_L - \frac{1}{B_C}\right), \quad (12)$$

where L and C are the inductance and capacitance offered by the patch elements on the dielectric substrate, respectively.

Two FSS layers as a top and bottom surfaces and connected through metallic vias will act as a π network. The normalized impedance of total structure is $Z_{FSS-SIW}$, viewing from input port with open-circuited output port of a π network given in equation (13)

$$Z_{FSS_SIW} = \frac{Z_a \cdot (Z_{via} + Z_b)}{Z_a + Z_b + Z_{via}}, \quad (13a)$$

where Z_{via} is the impedance offered by the metallic via and dielectric spacer whose EC is given below. The L_{via} and C_{via} are connected in parallel whose impedance is given as:

$$Z_{via} = j\left(\frac{\omega L_{via}}{n} - \frac{1}{\omega C_{via}}\right), \quad (13b)$$

where n represents the number of vias in one unit cell. Thin metallic vias will act as a wire inductor and inductance offered by the wire (L_{via}) is computed from equation (14) [26].

$$L_{via} = 2L\left\{\ln\left[\left(\frac{1 + \sqrt{1 + S^2}}{S}\right)\right] - \sqrt{1 + R^2} + \frac{\mu}{4} + S\right\} nH, \quad (14)$$

where $S = D_via/2L$, $R = \sqrt{1 + S^2}$, D_via and L are the diameter and length of the metallic vias. The length of metal vias is same as

https://doi.org/10.1017/S1759078718001678 Published online by Cambridge University Press

that of thickness of the dielectric substrate ($L = h$). The numerical value of via inductance computed with equation (14) is L_{via} = 0.724 mH and capacitance value is C_{via} = 2.39 pF which is computed using the relation $\varepsilon A/h$, where h is the spacing between two metallic plates (height of the substrate) and A is the plate area. The initial values of *D_via, K_via*, and design parameters of FSS are computed at the centre frequency of 10 GHz. The necessary design rules are considered to design the metallic vias [27, 28]. The described EC model is valid for all element shapes. Here, the metallic vias can suppress the propagation of EM interference through the gap between the two parallel conducting FSS layers and SIW vias. The relationship between *D_via* and *K_via* can be satisfied to eliminate inter-elemental effects as found in equation (15) [27].

$$K_via > D_via, \tag{15a}$$

$$(D_via/K_via) > 0.5, \tag{15b}$$

$$0.25 < \frac{K_via}{\lambda_c} < 0.05. \tag{15c}$$

The condition (15a) states that the spacing between metallic vias should be larger than the diameter of the via to facilitate the physical realization. The condition (15b) is required to neglect the leakage through SIW vias. The number of vias should not exceed 20 per wavelength as stated in (15c). It is worth to mention that diameter of vias should not exceed the width of FSS element.

To show the effectiveness of derived formulas, the real and imaginary parts of the normalized impedances *w.r.t* maximum value, of both SSL and JC FSS elements in conventional form and using SIW technology, are shown in Fig. 4. It can be observed that the impedance response of the structure with SIW technology is improved significantly. Hence, the better impedance matching is possible in wide frequency region, And thus results in improving the BW. The resonance occurs when the inductive impedance is equal to capacitive impedance of the structure, i.e. *real*(Z) = *imag*(Z) = 0 of the circuit, which shown in Fig. 4.

Finally, the corresponding voltage reflection coefficient of proposed FSS element with SIW technology "Γ" is expressed as:

$$\Gamma = \frac{Z_{FSS_SIW} - 1}{Z_{FSS_SIW} + 1}, \tag{16}$$

where $Z_{FSS-SIW}$ is the normalized impedance of the structure. The power transmitted due to grid array $|T|^2$is:

$$|T|^2 = 1 - |\Gamma|^2. \tag{17}$$

To show the efficacy of proposed EC mode for FSS with SIW technology, the results obtained with EC model are compared with an FDTD-based commercial full-wave simulation tool CST MWS. The unique feature of unit-cell boundary conditions with Floquet mode excitation is used to simulate the behavior of infinite FSS array. The results shown in Figs 5(a)–5(d) exhibit a good approximation between the analyzed FSS and FSS–SIW FSS elements using circuit model (ECM) and full-wave simulation. The structures are analyzed at *X*-band, all below figures are plotted on the scale from 4 to 16 GHz to observe the existence of higher

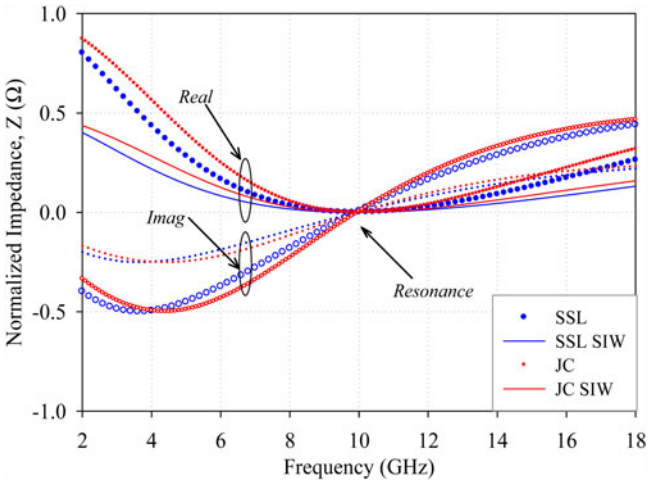


Fig. 4. Real and imaginary part of normalized impedance of SSL and JC in conventional form and proposed 2.5D base on SIW technology on R4003C substrate with thickness h = 0.81 mm.

order resonances. The reflection response shown in Figs 5(a) and 5(c) clearly shows the increment in their BW; whereas, the transmission parameters are presented in Figs 5(b) and 5(d), the −10 dB BW of the proposed FSS elements using SIW is improved significantly. The BW can further improve with proper tuning of the design parameters which is discussed in Section 3 of this paper. The EC method can give a knowledge of parametric effects such as dimensions of elements and dielectric parameters of substrate materials used in the design. Though, it is a powerful method to analyze the response of FSS structures with better accuracy and less CPU computation time (fraction of seconds); whereas, the simulation tools may take few minutes to hours depending on the structural complexity.

The structures are analyzed from 2 to 18 GHz to observe the existence of unwanted resonances. From the transmission curves presented in Fig. 5, the −10 dB fractional BW of the proposed FSS elements using SIW is improved in SSL from 3.44 to 4.75 GHz and in JC FSS from 1.9 to 3.17 GHz in *X*-band region, as compared with their conventional shape, respectively. In case of JC SIW element, fractional BW obtained using EC model is 4.3 GHz (8–12.3 GHz) which is 1.3 GHz more compared with its conventional form (8.6–11.6 GHz). While the simulation results show 3.17 GHz (8.4–11.57 GHz) BW, whereas in the conventional form it is only 1.17 GHz (8.9–10.9). Accordingly, the relative error of BW for EC model w.r.t full-wave simulation is 35%. The resonant frequency is observed at 10.01 GHz using EC model and at 10.10 GHz by using simulation. Hence, root-square-mean-error of resonant frequency is only 0.89%. However, it is worth to remind that the EC model can help to estimate the initial response of the structure. Even though it is a powerful method to analyze the response of FSS structures with better accuracy and less CPU computation time, the simulation tools may take few minutes to hours depending on the structural complexity. Once the initial parameters have identified, the final design can be obtained using full-wave simulations.

Apart from the conventional FSS, the proposed structures show a very stable response at different angle of incidence. It has been observed in conventional FSS that the resonance frequency shifts toward lower frequency regime (left side) as the angle of incidence rise from 0° to 70° as shown in Tables 1 and 2

https://doi.org/10.1017/S1759078718001678 Published online by Cambridge University Press

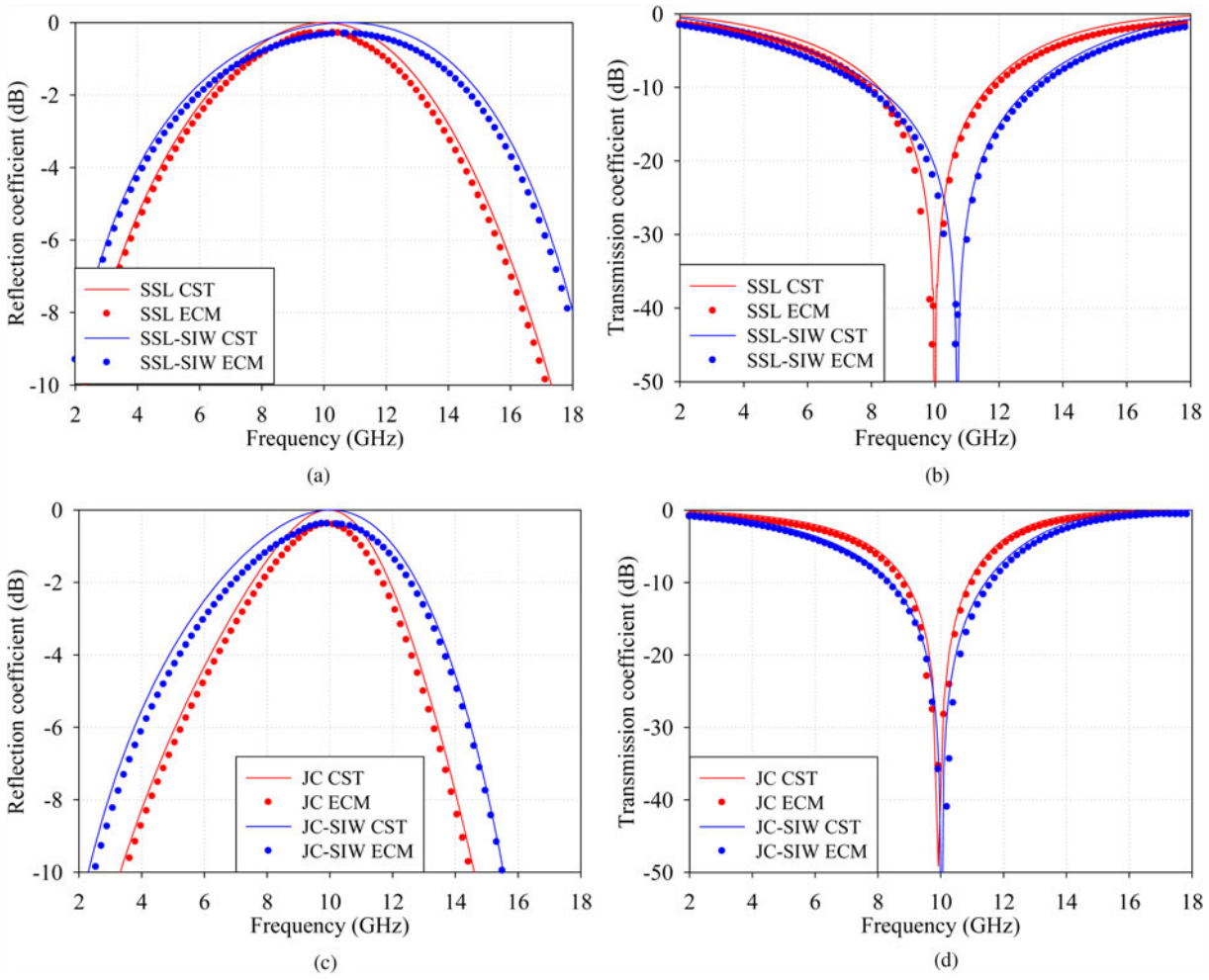


Fig. 5. EM-performance of FSS–SIW technology: (a) reflection coefficient comparison of SSL FSS and SSL–SIW FSS, (b) transmission coefficient comparison of SSL FSS and SSL–SIW FSS, (c) reflection coefficient comparison of JC FSS and JC–SIW FSS, (d) transmission coefficient comparison of JC FSS and JC–SIW FSS (bubbles show the response of FSS element with ECM and solid line shows the response with CST MWS).

Table 1. Effect of incident angle on the resonance performance of SSL

	Conventional form			Proposed form		
Incident angle, Deg	*fr*, GHz	Deviation, %	FBW, %	*Fr*, GHz	Deviation, %	FBW, %
0	10.0	0	33.72	10.0	0	62.14
10	9.88	−1.2	32.62	10.0	0	60.07
20	9.84	−1.6	32.54	9.96	−0.4	60.07
30	9.77	−2.3	32.15	9.95	−0.5	60.0
40	9.7	−3.0	33.15	9.9	−1.0	62.94
50	9.63	−3.7	36.68	9.85	−1.5	68.75
60	9.58	−4.2	43.22	9.82	−1.8	78.46
70	9.5	−5.0	61.05	9.77	−2.3	99.65

for SSL and JC FSS, respectively. The transmission and reflection characteristics of aforementioned FSS–SIW structures (loop and cross elements) at wide incident angles have been studied and presented in Figs 6(a)–(d), respectively. Very stable resonance characteristics for both TE and TM polarizations were observed at different angles of incidence. The frequency response of proposed SSL and JC elements using SIW over the conventional form is shown in Tables 1 and 2, respectively.

https://doi.org/10.1017/S1759078718001678 Published online by Cambridge University Press

Table 2. Effect of incident angle on the resonance performance of JC

	Conventional form			Proposed form		
Incident angle, Deg	*fr*, GHz	Deviation, %	FBW, %	*fr*, GHz	Deviation, %	FBW, %
0	10.0	0	20.2	10.0	0	30.0
10	9.90	−1.0	20.94	10.0	0	30.3
20	9.92	−0.8	21.54	10.0	0	30.71
30	9.88	−1.2	23.6	10.0	0	31.47
40	9.81	−1.9	24.97	9.87	−1.3	37.75
50	9.74	−2.6	30.9	9.80	−2.0	41.93
60	9.70	−3.0	37.42	9.75	−2.5	54.34
70	9.63	−3.7	52.37	9.72	−2.8	67.40

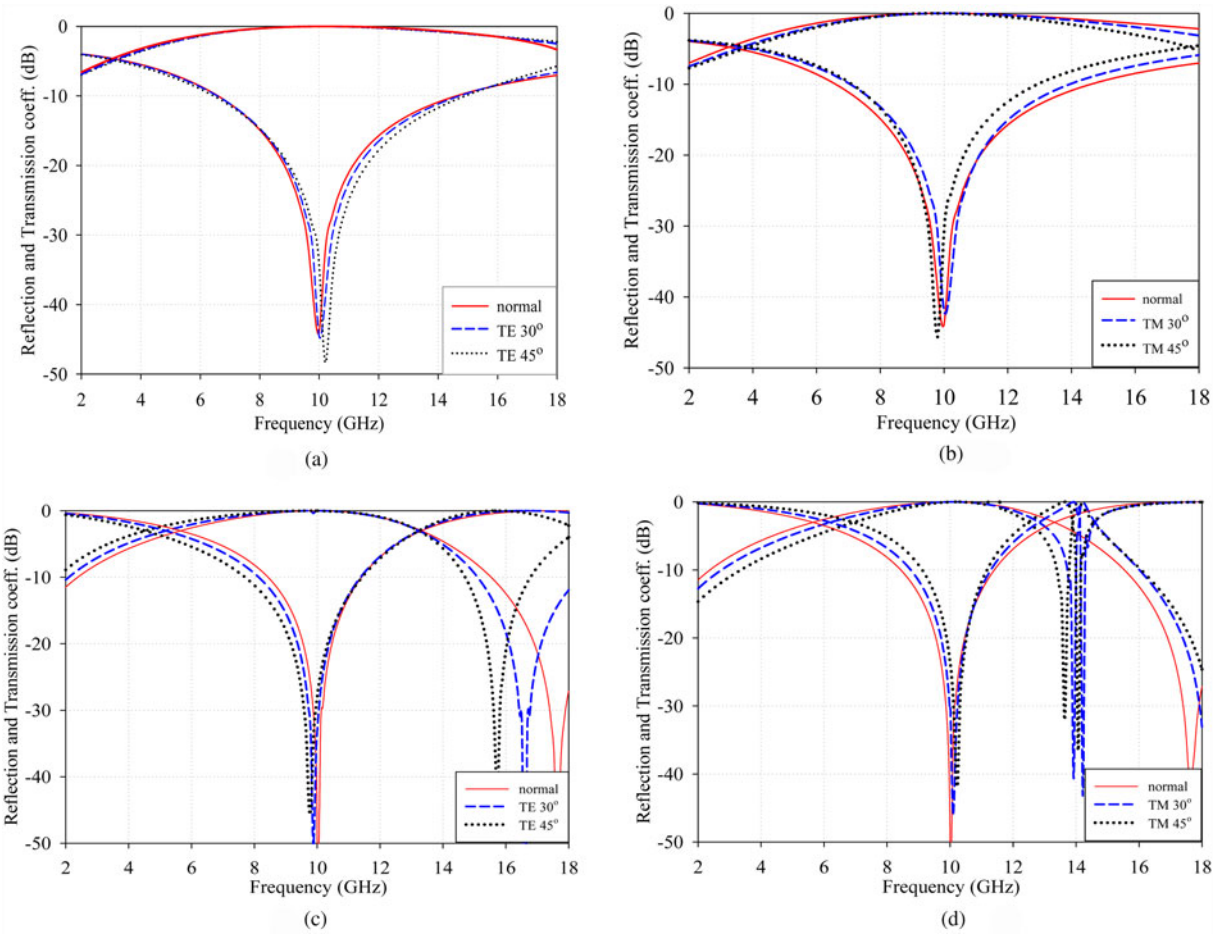


Fig. 6. Transmission and reflection coefficient of proposed FSS design at different angle of incidence: (a) SSL at TE polarization, (b) SSL at TM polarization, (c) JC at TE polarization, (d) JC at TM polarization.

EM design of FSS–SIW element

The FSS, owing to the presence of SIW metallic vias in structure, results in an increase of BW and stable response w.r.t polarization at a different angle of incidence is achieved. The addition of SIW vias improves the EM performance. The vias used here will develop virtually thick FSS screens without altering its resonance performance.

However, there can exist limitations on structural dimensions of FSS elements and metallic vias, which can alter the required EM performance. The effects of structural dimensions of conventional FSS elements have been extensively reported in the earlier literature. In the proposed structure, the effect of substrate height, dielectric constant, and SIW vias are the main parameters needed to be considered to study the resonance performance. Moreover,

https://doi.org/10.1017/S1759078718001678 Published online by Cambridge University Press

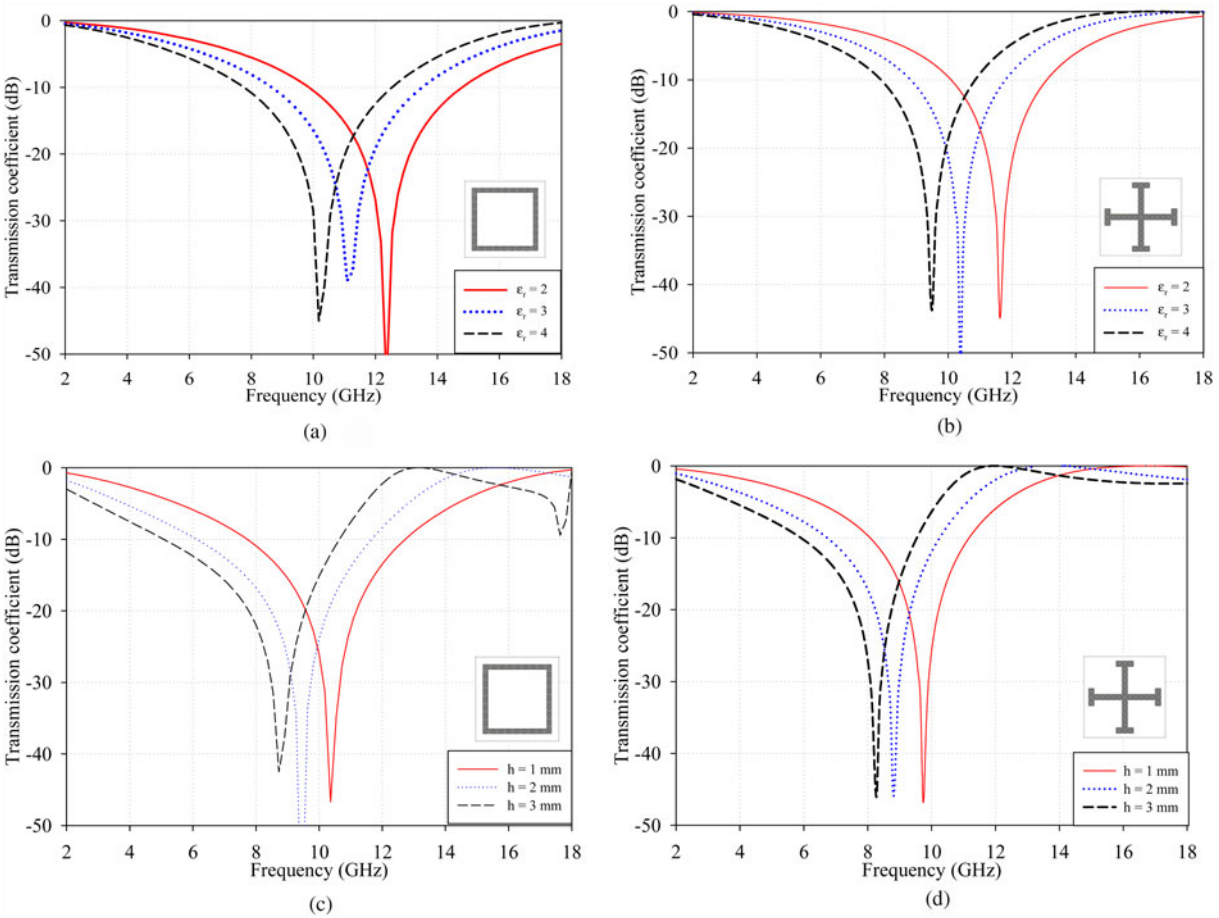


Fig. 7. Influence of dielectric substrate parameters on the transmission response: (a) effect of ε_r on SSL FSS–SIW, (b) effect of ε_r on JC FSS–SIW, (c) Effect of h on SSL FSS–SIW, (d) Effect of h on JC FSS–SIW.

in conventional form, the height of substrate and dielectric constant have contributed negligible effect. Whereas, in presented form, the dielectric spacer has been placed in between two FSS layers which act as a parallel plate capacitor ($C = \varepsilon_0\varepsilon_r/A$, where A is directly related to the height of the substrate h). The capacitance will act in parallel to the inductive impedance induced by the metallic vias that can change the expected performance. The study helps to understand the behavior of FSS element with design parameters.

Effect of dielectric substrate

The dielectric substrate is used for physical support to FSS element. It is not only providing the physical support, but also a crucial parameter in the design of FSS. This substrate can have a profound effect on *EM*-performance of the structure [1]. The influence of the substrate parameters such as dielectric constant and thickness has been studied here.

Dielectric constant

Dielectric constant is an important parameter in the design of FSS. In general two things may happen when a dielectric substrate is loaded to the FSS: one, the resonant frequency (f_0) changes, also changes the BW for a different angle of incidence. Second, the periodic structure gets infinite support with relative dielectric constant (ε_r). Since the structure has dielectric substrate in the center of two FSS layers, the resonant frequency shifts leftwards with a factor of $f_0/\sqrt{(\varepsilon_r + 1)/2}$. The variations in transmission coefficient as changing with dielectric constant are shown in Figs 7(a) and 7(b). From the observations made on the structures, it is found that different from its conventional form as ε_r increases, increases the capacitive impedance of the structures makes the improving and BW.

Thickness of dielectric substrate

Figures 7(c) and 7(d) show the variations in f_0 as the substrate thickness (h) increases. In established form, the substrate thickness have a negligible effect on the resonant and BW response of the structure. Different from conventional form, using SIW technology, the resonant curves shift toward the lower frequency regime. Hence, the substrate thickness of SIW has a primary effect on f_0 and BW whose effects cannot be ignored. Further increase in thickness, the proposed structure exhibits spectacular performance which cannot be found in the established form of FSS. The performance comparison of proposed FSS over conventional form at $h = 8.0$ mm is shown in Fig. 8. As thickness of the substrate approaches $\lambda/4$, the EM wane perturbations inside the structure lead to the occurrence of second higher order resonance, hence results in two strong stop bands at 9.26 and 15.86 GHz, respectively, with a very good passband in between them. In Fig. 8, the response of the proposed structure at the thickness of 8.0 mm (which is also equal to the height of the SIW vias)

https://doi.org/10.1017/S1759078718001678 Published online by Cambridge University Press

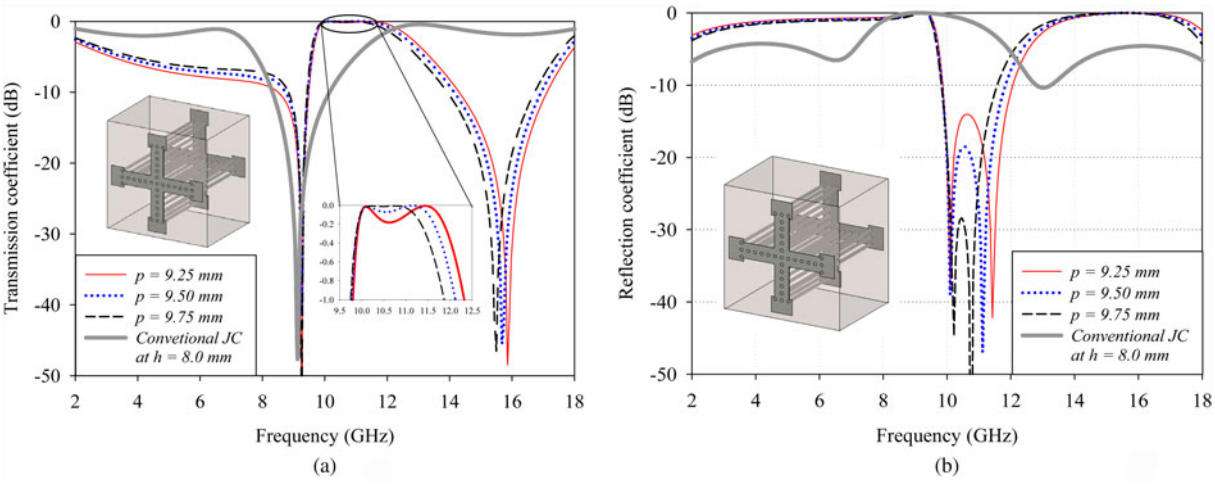


Fig. 8. Frequency response of proposed element at $h = 8$ mm at different cell size: (a) transmission, (b) reflection.

Table 3. Comparison of existing results with proposed structure

Ref. no.	Resonance frequency (in GHz)	Substrate thickness (mm)	Dielectric constant, ε_r	−10 dB relative BW (%)	Technique used
[4]	2.5, 3.0	0.8	4.4	22.2 at 3 GHz	Closely spaced meander lines on single side of a substrate
[5]	2.7	1.0	2.65	10.5	Design is composed of four spiral triangles connected in the middle of the unit cell symmetrically on single side of substrate
[10]	3.5	1.6	5.0	3.97	The unit cell consists of four spiral rectangular slots connected to a cross-line element at the middle on one side of substrate
[11]	4.0	1.0	2.65	18	The design consists of four symmetrical spiral patterns of metallic meander lines printed on single side of a substrate
[15]	6.5	2.4	4.6	7	A 3D four-legged loop element on a four-layer substrate
Proposed strongly coupled SSL	10.0	0.81	3.35	59.68	A novel double-layer square loop FSS strongly coupled with SIW via
Proposed strongly coupled JC	10.0	0.81	3.35	29.62	A novel double-layer JC FSS strongly coupled with SIW via

Table 4. Parametric effect on the resonance performance of SSL

		Conventional form			Proposed form		
Design parameter		*fr*, GHz	Deviation, %	FBW, %	*fr*, GHz	Deviation, %	FBW, %
Width of element, *w* (*mm*)	0.6	10.00	0	33.86	10.04	0	59.68
	0.8	10.75	7.5	36.61	11.2	12.0	63.22
	1.0	11.68	16.8	38.47	12.5	25.0	64.95
Substrate thickness, *h* (*mm*)	1	09.60	−4.0	34.5	9.77	−2.3	66.52
	2	09.10	−9.0	31.62	9.0	−10.0	81.68
	3	09.04	−9.6	27.57	8.44	−15.6	93.28
Substrate dielectric constant, ε_r	2	11.60	16.0	28.86	11.7	17.0	52.98
	3	10.42	4.2	32.134	10.51	5.1	57.88
	4	09.56	−4.4	34.82	9.63	−3.7	63.03

with different cell sizes has been presented. The substrate height is almost equal to $\lambda/4$ (quarter wavelength). The perturbation phenomena occur between the two metallic layers separated by the dielectric spacer. This effect results in the generation of second-order mode at higher frequency. As shown in Fig. 8(a), a higher order resonance can be seen at nearly 16 GHz on its

https://doi.org/10.1017/S1759078718001678 Published online by Cambridge University Press

Table 5. Parametric effect on the resonance performance of JC

Design parameter		Conventional form			Proposed form		
		fr, GHz	Deviation, %	FBW, %	*fr*, GHz	Deviation, %	FBW, %
Width of element, *w* (*mm*)	0.6	10.75	7.5	22.68	09.87	−1.3	29.06
	0.8	10.24	2.4	21.41	10.38	3.8	30.90
	1.0	09.73	−2.7	20.26	10.96	9.6	32.14
Substrate thickness, *h* (*mm*)	1	09.80	−2.0	20.89	09.73	−2.7	32.65
	2	09.50	−5.0	10.06	08.85	−11.5	41.60
	3	09.44	−5.6	15.77	08.30	−17.0	46.50
Substrate Dielectric constant, ε_r	2	11.60	16.0	17.86	11.61	16.1	26.20
	3	10.30	3.0	20.22	10.38	3.8	29.04
	4	09.37	−6.3	22.17	09.47	−2.6	29.06

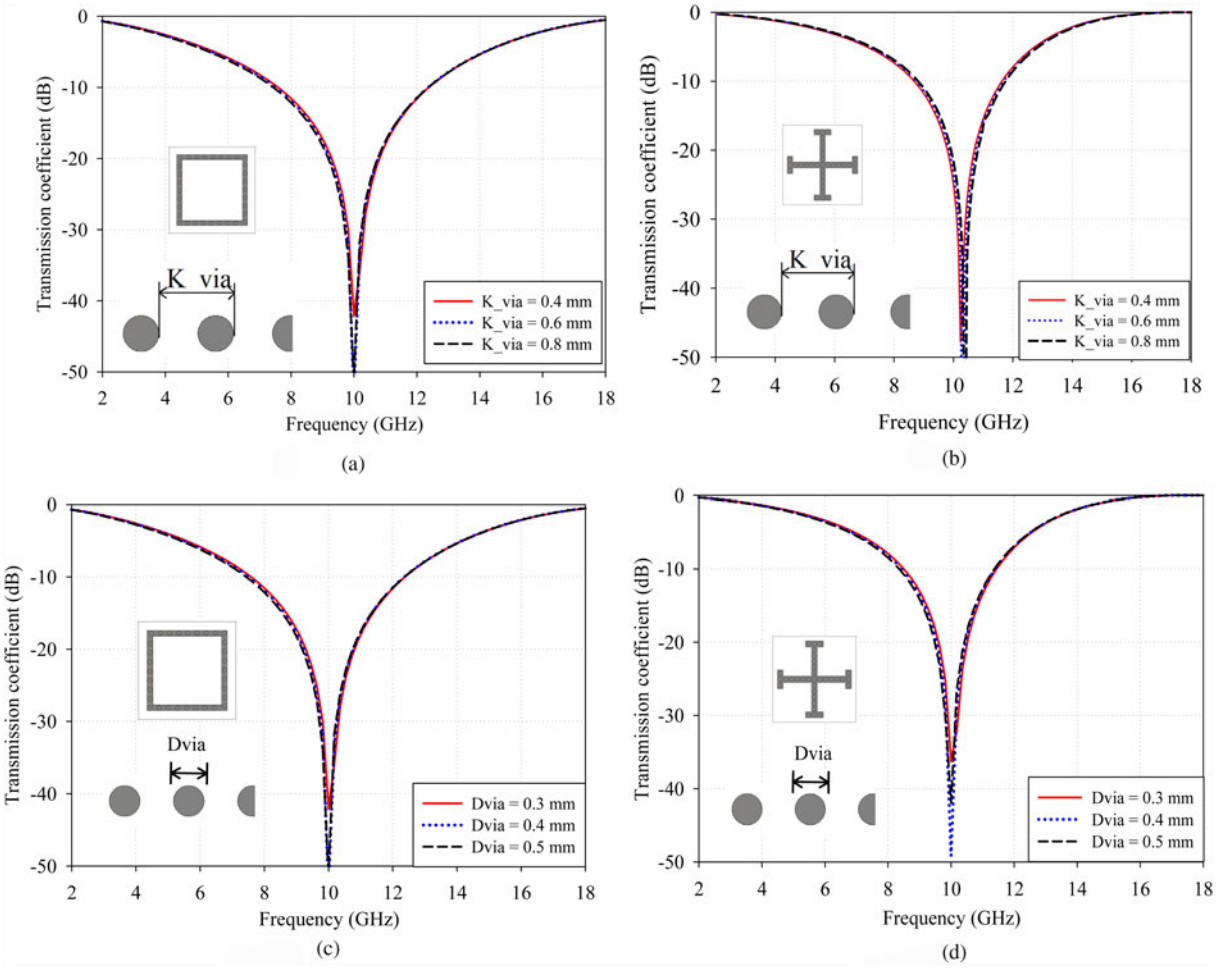


Fig. 9. Influence of metallic SIW vias parameters on the performance of transmission coefficient: via spacing on (a) SSL FSS–SIW, (b) JC FSS–SIW element. Via diameter on (c) SSL FSS–SIW, (d) JC FSS–SIW element.

transmission response. Consequently, there are two stopbands found at 9.0 and 16 GHz, respectively. Then there exists a strong pass band in between two stopbands from 9.8 to 12.3 GHz with fractional BW of 22.6% with better than 90% transmission efficiency. The corresponding reflection coefficient of the structure is shown in Fig. 8(b).

The extensive parametric study of proposed FSS proves the feasibilities of designing wideband FSS structures with stable

https://doi.org/10.1017/S1759078718001678 Published online by Cambridge University Press

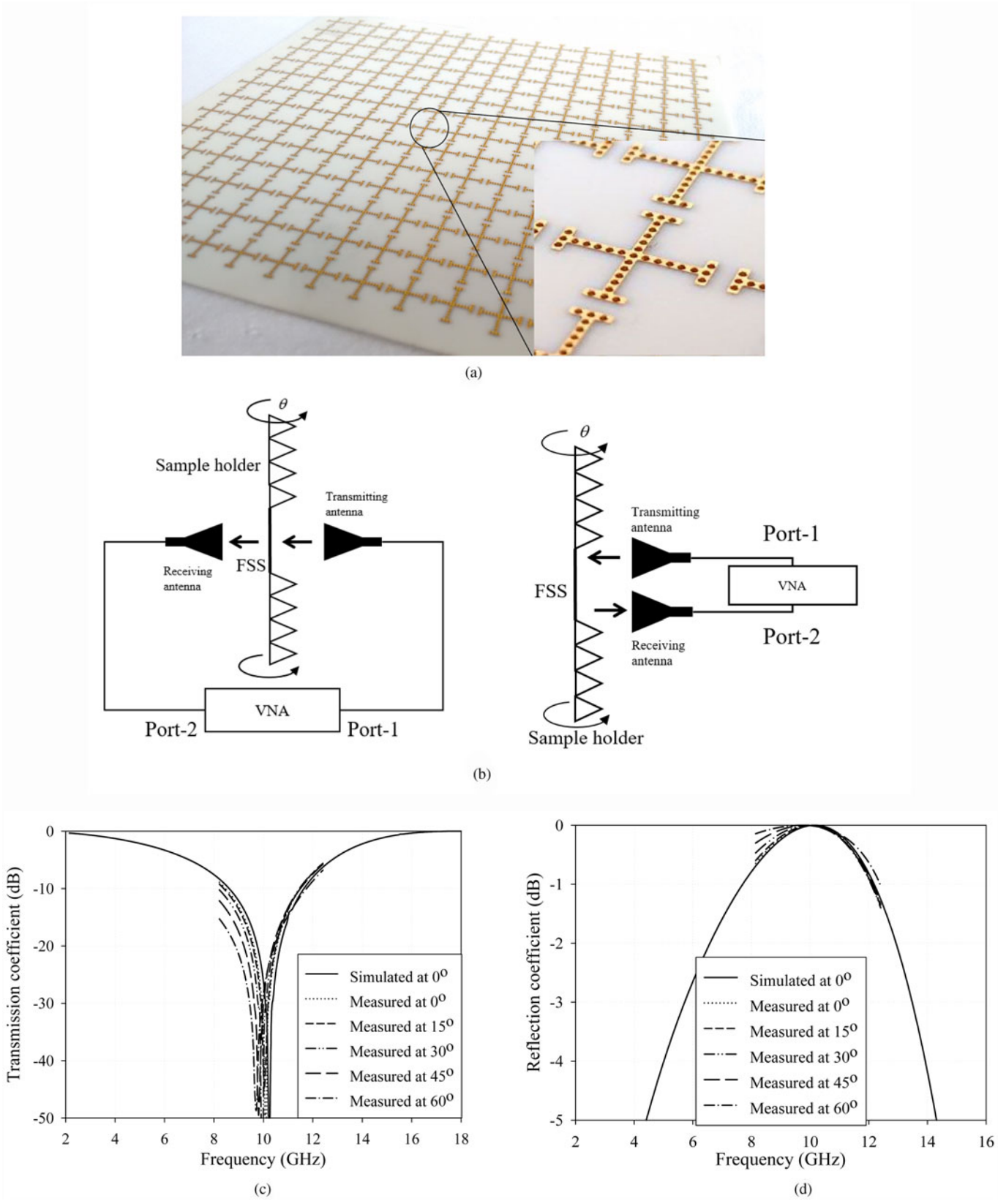


Fig. 10. Fabrication and experimental verification: (a) photograph of the fabricated prototype 16 × 14 array (inset shows the unit cell), (b) FSS measurement setup for transmission (left) and reflection (left) coefficient, (c) comparison of measured and simulated results transmission coefficient, (d) comparison of measured and simulated results reflection coefficient.

https://doi.org/10.1017/S1759078718001678 Published online by Cambridge University Press

resonance performance. It is well known that FSS is used as an infinite surface, where the weight of FSS plays an important role in practical applications. The proposed FSS has an advantage of lightweight because of the SIW cavities. Also, the size and thickness of the structure are $0.308\lambda_0$ and $0.027\lambda_0$, respectively, which is compact and ultrathin design suitable for real-time application without any further optimization. Moreover, it is also possible to realize 3D FSS elements with reduced weights using SIW cavity technology, which might be an interesting topic in future research.

Table 3 shows the comparison of literature results with the proposed structure. From the comparison, it is clear that the proposed 2.5D FSS exhibits improved BW at ultrathin thickness. Furthermore, the frequency response of the structure is very stable upto 60° compared with existing results.

Metallic vias

The metallic vias is the important design parameter of the proposed structure. The variations in the vias such as height, spacing, and diameter may affect the performance of FSS. For instance, the variation in the height of metallic vias in conventional form and proposed form is shown in Tables 4 and 5 for SSL and JC, respectively. Moreover, a better insight of vias (directly rated to height of substrate) has been presented in Fig. 8. For deep observation, the effect of vias such as spacing and diameter has been reported in the following sub-sections.

Spacing between vias

The metallic via spacing should satisfy the conditions given in Equation (15) to avoid the EM leakage through it. Based on the given conditions, the value of K_vas has been determined as 0.635 mm. The same value has been used in the entire analysis of both presented structures. For better understanding, to estimate the dependency of vias spacing on frequency response, a parametric study has been conducted on different design values of K_via at 0.4, 0.6, and 0.8 mm. Figures 9(a) and 9(b) show the transmission response of the proposed square loop and JC elements at different via spacing. It has been observed that the effect of via spacing within the considered limit is negligible.

Diameter of vias

The effect of connecting metallic vias is studied in this section. From Figs 9(c) and 9(d), it is clear that the effect of vias diameter on the performance of FSS is insignificant. The transmission curves are almost same as increasing the diameter from 0.3 to 0.5 mm. After all, care should be taken while choosing the diameter of vias, i.e. it should not exceed the width of conducting element. The inductance offered by the metallic post mainly depends on the length of via then in its diameter. The purpose of vias is to interconnect the two FSS elements placed on either side of the substrate. Hence, the diameter should not cross the limits of FSS element width which may lead to develop the higher order modes.

Fabrication and experimental verification

To prove the efficacy of analyzed results using EC method and full-wave simulation package, the proposed JC element with SIW vias structure has been fabricated using printed circuit board technology. A total of 16×14 cells are fabricated on 160 mm × 140 mm *R*04003*C* substrate with $\varepsilon_r = 3.38$ having a thickness of $h = 0.81$ mm. The conductive periodic JC FSS array has been printed on either side of the substrate material. Then, the vias are made by drilling the holes with a diameter of 0.4 mm from the top layer to the bottom layer through the substrate and then coated with a thin copper material (0.035 mm) which can enable a metallic contact between the two layers. The fabricated prototype is shown in Fig. 10(a). In this setup, a pair of standard gain horn antennas (8.2–12.4 GHz) is connected to port-1 (transmitter) and port-2 (receiver) of ZVA 24 network analyzer (100 MHz–24 GHz) from Rhode and Schwartz. The structure is kept at the center of a pyramidal absorber to suppress the edge effects of the sample as shown in Fig. 10(b). Finally, the transmission and reflection curves of both simulated and measured values are compared at normal 60° incidence angle as shown in Figs 10(c) and 10(d), respectively. It can be seen that the measurement results are good in agreement with the analyzed results.

Conclusion

An approach to improve the BW and angularly stable 2.5D FSSs using SIW technology is presented. Two basic 2.5D FSS elements viz. square loop (loop type) and JC (center-connected type) have been investigated to prove the enhancement in their BW using SIW technology using ECM for initial estimation, further the final structure is obtained with the help of full-wave simulations using CST MWS. The parametric effects on the transmission response of the structures have been studied and compared with that of conventional form. The results prove the improvement in BW and angular stability of the proposed structure. Moreover, the structure is more suitable for real-time applications because of its ultrathin thickness ($0.027\lambda_0$). Finally, the measured results of the fabricated prototype prove the advantages of proposed structural topology.

Further studies on the proposed structures can serve the stable resonance. Also, prove as an alternative to 2-D and 3-D FSS structures with better EM performance characteristics for aerospace applications with reduced payloads and EMI shielding.

Author ORCIDs. Krushna Kanth Varikuntla 0000-0002-7429-8386.

Acknowledgement. Authors would like to thank Dr. D. C. Pande, Eminent Scientist, DRDO-LRDE, and Dr. Shivnarayan, CSIR-NAL for their technical support and gratefully acknowledge the Rogers Corporation, AZ, USA for providing the dielectric samples used in this study.

References

[1] **Munk BA** (2000) *Frequency Selective Surfaces: Theory and Design*. New York: Wiley.

[2] **Li B and Shen Z** (2014) Dual-band bandpass frequency-selective structures with arbitrary band ratios. *IEEE Transactions on Antennas and Propagation* **62**, 5504–5512.

[3] **Kartal M, Golezani JJ and Doken B** (2017) A triple band frequency selective surface design for GSM systems by utilizing a novel synthetic resonator. *IEEE Transactions on Antennas and Propagation* **65**, 2724–2727.

[4] **Ghosh S and Srivastava KV** (2017) An angularly stable dual-band FSS with closely spaced resonances using miniaturized unit cell. *IEEE Microwave and Wireless Components Letters* **27**, 218–220.

[5] **Liu N, Sheng XJ and Fan JJ** (2016) A compact miniaturized frequency selective surface with stable resonant frequency. *Progress In Electromagnetics Research* **62**, 17–22.

https://doi.org/10.1017/S1759078718001678 Published online by Cambridge University Press

[6] **Chaharmir MR and Shaker J** (2015) Design of a multilayer X-/Ka-band frequency-selective surface-backed reflect array for satellite applications. *IEEE Transactions on Antennas and Propagation* **63**, 1255–1262.
[7] **Oraizi H and Afsahi M** (2007) Analysis of planar dielectric multilayers as FSS by Transmission Line Transfer Matrix Method (TLTMM). *Progress In Electromagnetics Research* **74**, 217–240.
[8] **Li M and Behdad N** (2013) Wideband true-time-delay microwave lenses based on metallo-dielectric and all-dielectric lowpass frequency selective surfaces. *IEEE Transactions on Antennas and Propagation* **61**, 4109–4119.
[9] **Shivnarayan and Jha RM** (2015) Electromagnetic techniques and design strategies for FSS structure applications [antenna applications corner]. *IEEE Transactions on Antennas and Propagation* **57**, 135–158.
[10] **Yang G, Zhang T, Li W and Wu Q** (2010) A novel stable miniaturized frequency selective surface. *IEEE Antennas and Wireless Propagation Letters* **9**, 1018–1021.
[11] **Yan M, Qu S, Wang J, Zhang J, Zhang A, Xia S and Wang W** (2014) A novel miniaturized frequency selective surface with stable resonance. *IEEE Antennas and Wireless Propagation Letters* **13**, 639–641.
[12] **Munk BA, Luebbers R and Mentzer CA** (1971) Breakdown of periodic surfaces at microwave frequencies, ElectroScience Lab., Dept. Elect. Eng., Ohio State Univ., Columbus, OH, Tech. Rep., 1971, 2989–2981.
[13] **Liu CH, Booske JH and Behdad N** (2014) Investigating failure mechanisms in high-power microwave frequency selective surfaces, IEEE Antennas Propag. Society Int. Symp. (APSURSI), Memphis, TN, USA, 06–11 July 2014.
[14] **Lu ZH, Liu PG and Huang XJ** (2012) A novel three-dimensional frequency selective structure. *IEEE Antennas and Wireless Propagation Letters* **11**, 588–591.
[15] **Lee IG and Hong IP** (2014) 3D frequency selective surface for stable angle of incidence. *Electronics Letters* **50**, 423–424.
[16] **Joardar K** (1995) Comparison of SOI and junction isolation for substrate crosstalk suppression in mixed mode integrated circuits. *Electronics Letters* **31**, 1230–1231.
[17] **Luo GQ, Hong W, Hao ZC, Liu B, Li WD, Chen JX, Zhou HX and Wu K** (2005) Theory and experiment of novel frequency selective surface based on substrate integrated waveguide technology. *IEEE Transactions on Antennas and Propagation* **53**, 4035–4043.
[18] **Xu RR, Zong ZY, Yang G and Wu W** (2008) Loaded frequency selective surfaces using substrate integrated waveguide technology. *Microwave and Optical Technology Letters* **50**, 3149–3152.
[19] **Luo GQ, Hong W, Lai QH and Sun LL** (2008) Frequency-selective surfaces with two sharp sidebands realised by cascading and shunting substrate integrated waveguide cavities. *IET Microwaves, Antennas & Propagation* **2**, 23–27.
[20] **Qi NN, Gong SX, Zhang YJ and Liu JF** (2008) Reducing bandwidth of FSS using substrate integrated waveguide technology. *Journal of Electromagnetic Waves and Applications* **22**, 2087–2096.
[21] **Xi CZ, Hong W, Wu K, Hong JT, Hao ZC, Chen JX, Zhou HX and Zhou H** (2014) Design of a bandwidth-enhanced polarization rotating frequency selective surface. *IEEE Transactions on Antennas and Propagation* **62**, 940–944.
[22] **Mollaei MSM** (2017) Narrowband configurable polarization rotator using frequency selective surface based on circular substrate-integrated waveguide cavity. *IEEE Antennas and Wireless Propagation Letters* **16**, 1923–1926.
[23] **Winkler SA, Hong W, Bozzi M and Wu K** (2010) Polarization rotating frequency selective surface based on substrate integrated waveguide technology. *IEEE Transactions on Antennas and Propagation* **58**, 1202–1213.
[24] **Ferreira D, Caldeirinha RFS, Cuiñas I and Fernandes TR** (2015) Square loop and slot frequency selective surfaces study for equivalent circuit model optimization. *IEEE Transactions on Antennas and Propagation* **63**, 3947–3955.
[25] **Langley RJ and Drinkwater AJ** (1982) Improved empirical model for the Jerusalem cross, in microwaves, optics and antennas. *IEE Proceedings H* **129**, 1–6.
[26] **Grover FW** (2004) *Inductance Calculations*. Dover Publications, New York.
[27] **Deslandes D and Wu K** (2006) Accurate modeling, wave mechanisms, and design considerations of a substrate integrated waveguide. *Microwave Theory and Techniques, IEEE Transactions on* **54**, 2516–2526.
[28] **Krushna Kanth V and Raghavan S** (2018) Ultrathin design and implementation of planar and conformal polarisation rotating frequency selective surface based on SIW technology. *IET Microwaves, Antennas & Propagation* **12**, 1939–1947.



V Krushna Kanth received his B.Tech. degree from JNTUA, Andhra Pradesh, India, in 2012 and M.Tech. degree in Electronics Engineering from Pondicherry University, India, in 2015. He is the student member of IEEE and EuMA. He has research experience of 1 year at Centre for Electromagnetics (CEM) of CSIR-National Aerospace Laboratories (CSIR-NAL), Bangalore, India. He is presently a Ph.D. research scholar at the Department of Electronics and Communication Engineering, National Institute of Technology Tiruchirappalli, India. He has published more than 10 research papers and co-authored a Springer brief. His current area of research interest includes frequency-selective surfaces, metamaterials, radome, absorbing structures, and RCS field computation.



S Raghavan is a senior professor at the Department of Electronics and Communication Engineering, National Institute of Technology Tiruchirappalli, India. He was awarded Ph.D. degree from IIT-Delhi, India in 2001. He has 35 years of educational activity and research experience in the area of RF and microwave. He is a recipient of the Best Teacher Award for the year 2007–08, Best Faculty Award for Electrical and Electronics division (P. K. Das Memorial Award) for the year 2010–11, Life Time Achievement in Microwave Engineering, Honorary Fellowship of Ancient Sciences and Archeological Society of India. He is a senior member (SM) in IEEE-MTT, EMBS, and CSI; Fellow in IETE, FIE, BESI, ATMS; and Life Member (LM) in ISTE, ISSS, SEMCE, MRSI, IATLIS, ILS, NPC, IAMI, BMES, SBAO, STERM, ASI. Dr. Raghavan has authored or co-authored more than 500 scientific research papers and technical reports.

https://doi.org/10.1017/S1759078718001678 Published online by Cambridge University Press